SCIENTIFIC REPORTS

OPEN

Monocyte-lymphocyte cross-communication via soluble CD163 directly links innate immune system activation and adaptive immune system suppression following ischemic stroke

Received: 2 June 2017
Accepted: 19 September 2017
Published online: 11 October 2017

Grant C. O'Connell[1,2], Connie S. Tennant[1], Noelle Lucke-Wold[1], Yasser Kabbani[3], Abdul R. Tarabishy[3], Paul D. Chantler[4,5] & Taura L. Barr[1,6,7]

CD163 is a scavenger receptor expressed on innate immune cell populations which can be shed from the plasma membrane via the metalloprotease ADAM17 to generate a soluble peptide with lympho-inhibitory properties. The purpose of this study was to investigate CD163 as a possible effector of stroke-induced adaptive immune system suppression. Liquid biopsies were collected from ischemic stroke patients (n = 39), neurologically asymptomatic controls (n = 20), and stroke mimics (n = 20) within 24 hours of symptom onset. Peripheral blood ADAM17 activity and soluble CD163 levels were elevated in stroke patients relative to non-stroke control groups, and negatively associated with post-stroke lymphocyte counts. Subsequent *in vitro* experiments suggested that this stroke-induced elevation in circulating soluble CD163 likely originates from activated monocytic cells, as serum from stroke patients stimulated ADAM17-dependant CD163 shedding from healthy donor-derived monocytes. Additional *in vitro* experiments demonstrated that stroke-induced elevations in circulating soluble CD163 can elicit direct suppressive effects on the adaptive immune system, as serum from stroke patients inhibited the proliferation of healthy donor-derived lymphocytes, an effect which was attenuated following serum CD163 depletion. Collectively, these observations provide novel evidence that the innate immune system employs protective mechanisms aimed at mitigating the risk of post-stroke autoimmune complications driven by adaptive immune system overactivation, and that CD163 is key mediator of this phenomenon.

Stroke triggers a systemic inflammatory response which results in a dramatic shift in the phenotype of the peripheral immune system. The innate arm of the peripheral immune system undergoes rapid activation, a phenomenon which results in significant elevations in circulating neutrophil and monocyte counts in the hours following onset[1,2]. Conversely, the adaptive arm of the peripheral immune system shifts into a state of suppression, often characterized by a prolonged period of lymphopenia and limited antigen responsiveness[2–4]. While the pathophysiological role of the innate immune response to stroke has been long appreciated, a growing body of evidence suggests that the adaptive immune response to stroke also critically influences patient outcome.

[1]Center for Basic and Translational Stroke Research, Robert C. Byrd Health Sciences Center, West Virginia University, Morgantown, West Virginia, USA. [2]Department of Pharmaceutical Sciences, School of Pharmacy, West Virginia University, Morgantown, WV, USA. [3]Department of Neuroradiology, Ruby Memorial Hospital, Morgantown, WV, USA. [4]Center for Cardiovascular and Respiratory Sciences, Robert C. Byrd Health Sciences Center, West Virginia University, Morgantown, West Virginia, USA. [5]Division of Exercise Physiology, School of Medicine, West Virginia University, Morgantown, West Virginia, USA. [6]School of Nursing, West Virginia University, Morgantown, West Virginia, USA. [7]Valtari Bio Incorporated, Morgantown, WV, USA. Correspondence and requests for materials should be addressed to G.C.O. (email: goconnell.wvu@gmail.com)

It is likely that the state of adaptive immune suppression which develops in response to stroke serves to limit the possibility of an autoimmune response as the blood brain barrier becomes disrupted, and peripheral populations of lymphoid cells become exposed to unfamiliar central nervous system (CNS) peptides via the lesional and lymphatic accumulation of activated innate antigen presenting cells loaded with neural antigens[5,6]. Expectedly, heightened adaptive immune activity immediately following stoke has been shown to prolong the inflammatory state and promote secondary tissue damage, factors which can ultimately contribute to poor prognosis[6,7]. While the state of adaptive immune suppression is acutely protective, if prolonged, it can constitute a significant detriment to recovery[8–12]. Patients which display prolonged adaptive immune suppression following stroke become highly susceptible to post-stroke infection[13–16], which is one of the leading causes of death in the post-acute phase of care[9]. Despite the fact that it is becoming increasingly evident that this delicate balancing act between maintenance of self-tolerance and pathogen susceptibility plays a significant role in recovery, the mechanisms which drive the peripheral adaptive immune response to stroke are not yet fully understood.

CD163 is a membrane-bound scavenger receptor for extracellular hemoglobin which is believed to be expressed exclusively within the innate immune system[17], where it is predominantly found on monocytes and macrophages[18], and to a lesser extent on neutrophils[19]. Various stimuli can trigger CD163 ectodomain shedding via cleavage by the metalloprotease ADAM metallopeptidase domain 17 (ADAM17)[20,21], resulting in generation of a soluble truncated peptide (sCD163) which has been shown in multiple studies to directly interact with lymphocytes and inhibit antigen-induced proliferation[22–24]. Interestingly, genome-wide transcriptomic screening performed by our group recently identified CD163 as being robustly up-regulated in the peripheral blood of ischemic stroke patients within hours of symptom onset[25]. Furthermore, other groups have reported heightened ADAM17 activity in animal models of ischemic brain injury[26–28], as well as stroke-induced increases in peripherally circulating levels of other ADAM17 substrates such as tumor necrosis factor alpha (TNFα) in human subjects[29,30]. Therefore, it is possible that stroke induces a rise in peripherally circulating levels of sCD163 via coordinate increases in CD163 expression and ADAM17 activity; such a rise in sCD163 levels could subsequently contribute to suppression of the adaptive immune system via the inhibitory effects of sCD163 on lymphocyte activity. Thus, the primary objective of this study was to investigate sCD163 as a potential modulator of post-stroke adaptive immune suppression.

Results

Clinical and demographic characteristics. A cohort of 39 ischemic stroke patients was recruited along with two control groups, the first consisting of 20 neurologically asymptomatic subjects, and the second consisting of 20 acute stroke mimics. Ischemic stroke patients were significantly older than both neurologically asymptomatic controls and stroke mimics. Relative to neurologically asymptomatic controls, ischemic stroke patients displayed a more prevalent history of myocardial infarction and atrial fibrillation, and a higher percentage reported as taking anticoagulatory medications. Conversely, ischemic stroke patients were relatively well matched with stroke mimics in terms of all recorded cardiovascular disease risk factors, comorbidities, and medication status (Table 1).

ADAM17 activity and sCD163 levels are elevated in the peripheral blood following stroke. In order to determine whether stroke drives an increase in peripheral sCD163 production *in vivo*, peripheral venous blood was collected within 24 hours of symptom onset, and expression of ADAM17 and CD163 was assessed at both the RNA and protein level using a combination of qRT-PCR, enzyme activity assay, and ELISA. Transcriptional levels of both ADAM17 and sCD163 were significantly elevated in the whole blood of ischemic stroke patients relative to that of both control groups independently of age (Fig. 1A,B). Protein assays supported these observations, as ischemic stroke patients displayed significantly heightened cellular ADAM17 activity in peripheral blood total hemocyte fractions (Fig. 1C), as well as significantly elevated plasma levels of sCD163 (Fig. 1D), once again in an age-independent fashion.

Expectedly, ADAM17 mRNA expression, CD163 mRNA expression, cellular TACE activity, and sCD163 levels were significantly positively correlated across the collective patient population, allowing us to summarize the peripheral activity of the sCD163 production pathway in terms of a single composite variable using principal components analysis (Fig. 1E); this composite variable was positively associated with injury severity in terms of both the National Institutes of Health stroke scale (NIHSS) and infarct volume (Fig. 1F,G). While our relatively small sample size and the variability inherent to such measures of injury status kept these associations from reaching statistical significance, these relationships tentatively inferred that the sCD163 production pathway is directly responsive to stroke pathology.

Taken as a whole, these collective observations provided associative evidence supporting our hypothesis that stroke induces a peripheral rise in sCD163 levels via increased ADAM17 activity.

sCD163 levels are negatively associated with post-stroke lymphocyte counts. To explore whether the elevations in sCD163 levels which we observed in ischemic stroke play a role in modulation of the stroke-induced peripheral immune response *in vivo*, we assessed the relationship between circulating sCD163 levels and post-stroke leukocyte counts within the ischemic stroke group. Plasma sCD163 levels were significantly negatively associated with post-stroke absolute lymphocyte counts (Fig. 2A), as well as significantly positively associated with both absolute monocyte counts and absolute neutrophil counts (Fig. 2B,C). Collectively, these results provided *in vivo* associative evidence which supported our hypothesis that stroke-induced increases in myeloid-derived circulating sCD163 may contribute to post-stroke suppression of the adaptive immune system.

Stroke-induced circulating factors trigger monocytic sCD163 production *in vitro*. Next, we wanted to determine the direct effects of the post-stroke peripheral inflammatory milleu on ADAM17-mediated sCD163 shedding by peripheral innate immune cell populations. To do this, primary neutrophil and monocyte

	Group:			p-value:		
	Asymptomatic (A; n = 20)	Stroke Mimic (SM; n = 20)	Ischemic Stroke (IS; n = 39)	Main Test	A vs. IS	SM vs. IS
[a]Age (*mean* ± *SD*)	58.6 ± 11.1	58.0 ± 17.0	73.1 ± 13.3	<0.001*	<0.001*	<0.001*
[b]Female *n* (%)	15 (75.0)	9 (45.0)	25 (64.1)	0.153	—	—
[a]NIHSS (*mean* ± *SD*)	0.0 ± 0.0	4.7 ± 4.9	8.6 ± 7.5	<0.001*	<0.001*	0.041*
[b]Family history of stroke *n* (%)	11 (55.0)	5 (25.0)	15 (38.5)	0.014*	0.549	0.778
[b]Hypertension *n* (%)	15 (75.0)	17 (85.0)	32 (82.1)	0.756	—	—
[b]Dyslipidemia *n* (%)	8 (40.0)	13 (65.0)	16 (41.0)	0.199	—	—
[b]Diabetes *n* (%)	2 (10.0)	7 (35.0)	8 (20.5)	0.188	—	—
[b]Previous stroke *n* (%)	1 (5.00)	5 (25.0)	7 (17.9)	0.221	—	—
[b]Atrial fibrillation *n* (%)	0 (00.0)	3 (15.0)	13 (33.3)	0.004*	0.005*	0.432
[b]Myocardial infarction *n* (%)	0 (00.0)	6 (30.0)	11 (28.2)	0.014*	0.021*	1.000
[b]Hypertension medication *n* (%)	14 (70.0)	16 (80.0)	27 (69.2)	0.723	—	—
[b]Diabetes medication *n* (%)	2 (10.0)	6 (30.0)	8 (20.5)	0.309	—	—
[b]Cholesterol medication *n* (%)	6 (30.0)	12 (60.0)	14 (35.9)	0.123	—	—
[b]Anticoagulant or antiplatelet *n* (%)	1 (5.00)	12 (60.0)	23 (59.0)	<0.001*	<0.001*	1.000
[b]Current smoker *n* (%)	1 (5.00)	2 (10.0)	13 (33.3)	0.023*	0.043*	0.127

Table 1. Clinical and demographic characteristics. [a]Means compared via one-way ANOVA with subsequent planned group-wise comparisons using Bonferroni-corrected two-sample two-tailed t-test; [b]Proportions compared via 2 × 3 Fisher's exact test with subsequent planned group-wise comparisons using Bonferroni-corrected 2 × 2 Fisher's exact test; NIHSS, National Institutes of Health stroke scale; SD, standard deviation.

cultures generated from the peripheral blood of twelve healthy donors (Supplementary Table 1) were treated with pooled serum samples derived from a subset of ten ischemic stroke patients, ten neurologically asymptomatic controls, and ten stroke mimics which were relatively well matched in terms of clinical and demographic characteristics (Table 2). Serum incubation was performed in both the presence and absence of Marimastat, a broad-spectrum metalloproteinase inhibitor which is highly active against ADAM17, and cellular ADAM17 activity and sCD163 production were assessed following three hours of treatment.

Generally, neutrophil cultures appeared phenotypically identical across all conditions when visually inspected following treatment (Fig. 3A). ADAM17 activity did appear to be elevated in neutrophil cultures treated with serum obtained from ischemic stroke patients relative to those treated with serum obtained from both neurologically asymptomatic controls and stroke mimics, however this increase was not statistically significant (Fig. 3B). Overall, neutrophil cultures appeared to generate relatively little sCD163, although a limited number of cultures treated with ischemic stroke serum did appear to exhibit increased sCD163 production in response to treatment. This effect was not widespread however, and no statistically significant differences were observed in sCD163 production between cultures treated with ischemic stroke serum and those treated with serum from control groups (Fig. 3C). A second independent experiment using pooled serum samples derived from a separate sub-set of subjects (Supplementary Table 2) yielded similar results (Supplementary Figure 1).

Counter to what was observed in terms of neutrophil cultures, there were striking visual differences between monocyte cultures treated with serum derived from ischemic stroke patients and those treated with serum derived from control groups. Cultures treated with control serum displayed a mix of adherent and semi-adherent cells, however several cultures incubated with ischemic stroke serum contained large patches of cells which appeared highly adherent with prominent cytoplasmic vacuoles classically characteristic of a shift towards an activated phenotype (Fig. 4A). This phenomenon was quantifiable via image-based analysis, as point counting revealed that cultures treated with ischemic stroke serum contained a significantly greater number of adherent cells (Fig. 4B), as well as a significantly greater number of cells containing clearly defined vacuolar structures (Fig. 4C), in comparison to cultures treated with serum from control groups. Furthermore, cellular ADAM17 activity was significantly elevated in cultures treated with ischemic stroke serum relative to those treated with serum from control groups (Fig. 4D), and supernatants recovered from cultures treated with ischemic stroke serum contained significantly higher concentrations of monocyte-derived sCD163 (Fig. 4E). Expectedly, the increase in monocytic sCD163 production which we observed upon stimulation with ischemic stroke serum was largely ablated by treatment with Marimastat (Fig. 4E), inferring that it was generated via the canonical sCD163 pathway involving ADAM17. Once again, similar results (Supplementary Figure 2) were observed in a second independent experiment using pooled serum samples derived from a separate sub-set of subjects (Supplementary Table 2).

Collectively, these observations demonstrate that soluble factors present in peripheral circulation following ischemic stroke have the capacity to trigger ADAM17-dependant sCD163 shedding from peripheral blood monocytes, however likely not from neutrophils.

Stroke-induced elevations in circulating sCD163 suppress lymphocyte proliferation *in vitro*. Lastly, we wanted to determine the direct effect of post-stroke-elevations in circulating sCD163 levels on the capacity of the peripheral blood to support lymphocyte proliferation. To do this, primary lymphocyte cultures derived from healthy donors (Supplementary Table 1) were stimulated to proliferate using

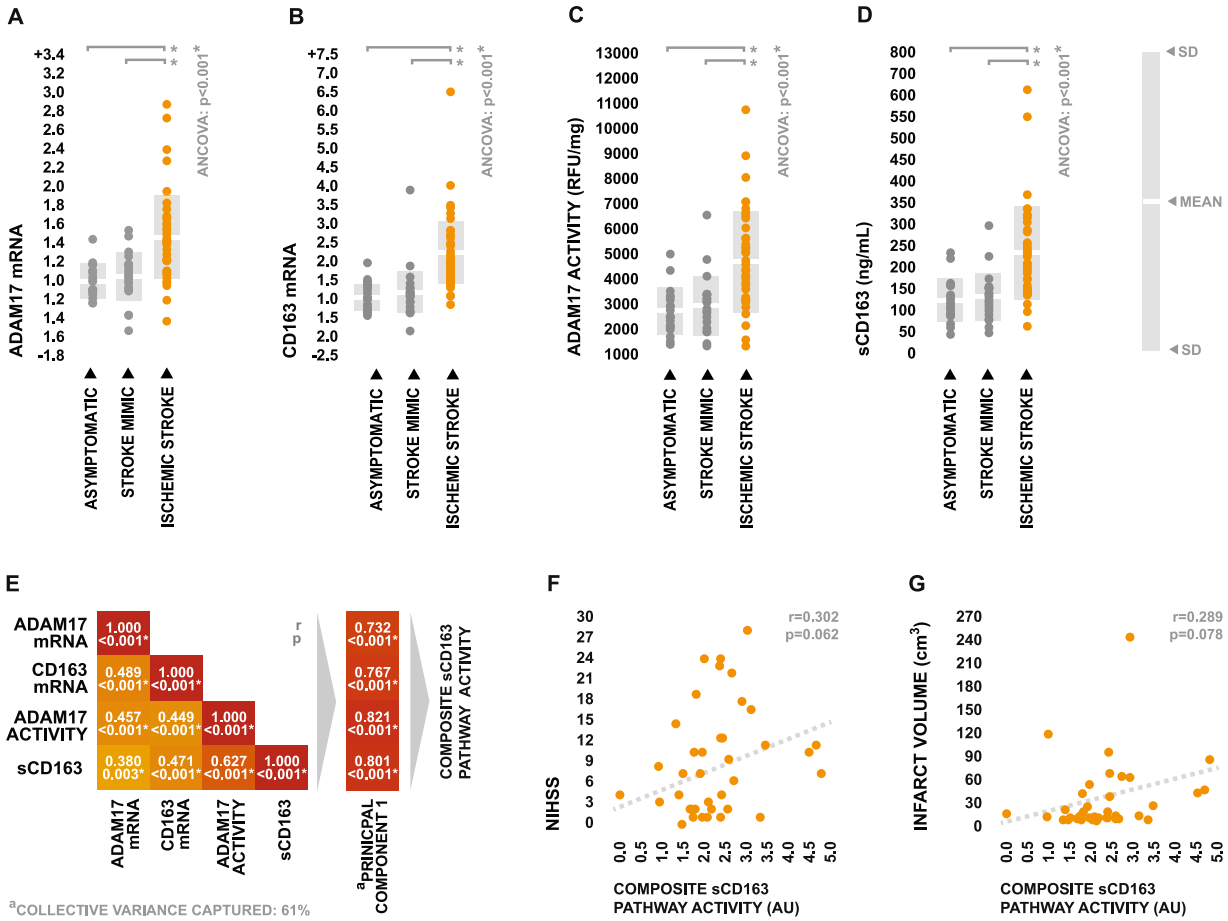

Figure 1. ADAM17 and CD163 expression in the peripheral blood following ischemic stroke. (**A**–**D**) Total ADAM17 mRNA expression, total CD163 mRNA expression, total cellular ADAM17 activity, and plasma sCD163 concentrations in peripheral blood biopsied from ischemic stroke patients, acute stroke mimics, and neurologically asymptomatic controls. mRNA expression values are presented as linearly-transformed values scaled relative to the mean of the asymptomatic control group. Inter-group comparison of means was performed using one-way ANCOVA with age as a covariate; in the case of a significant test, subsequent planned group-wise comparisons of age-adjusted values were performed via Bonferroni-corrected two-sample two-tailed t-test. ANCOVA was performed using log-transformed data in order to meet homogeneity of variance assumptions. (**E**) Correlation matrix depicting the group-wide collective relationships between peripheral blood ADAM17 mRNA expression, CD163 mRNA expression, ADAM17 activity, and sCD163 levels, along with the loadings of the single principal component used to summarize sCD163 pathway activity. Strength of correlations were tested using Pearson's r and p-values were adjusted for multiple tests via the Bonferroni correction. (**F**–**G**) Relationships between sCD163 pathway activity and injury severity as determined by NIHSS and infarct volume within the ischemic stroke group. Strength of correlations were tested using Spearman's rho.

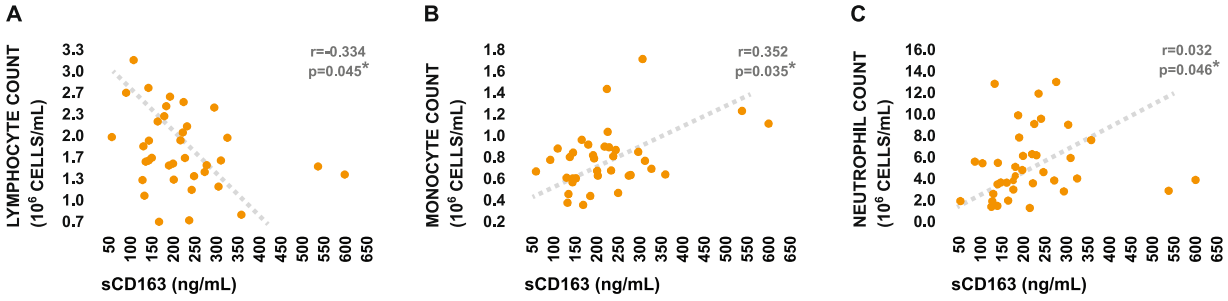

Figure 2. Relationship between plasma sCD163 levels and post-stroke peripheral immune status. (**A**–**C**) Relationships between plasma sCD163 levels and absolute lymphocyte counts, absolute monocyte counts, and absolute neutrophil counts in the peripheral blood of ischemic stroke patients. Strength of correlational relationships were tested via Spearman's rho.

	Group:			p-value:		
	Asymptomatic (A; n = 10)	Stroke Mimic (SM; n = 10)	Ischemic Stroke (IS; n = 10)	Main Test	A vs. IS	SM vs. IS
[a]Age (*mean* ± *SD*)	57.5 ± 11.1	56.4 ± 17.1	63.5 ± 14.3	0.536	—	—
[b]Female *n* (%)	8 (80.0)	5 (50.0)	5 (50.0)	0.348	—	—
[a]NIHSS (*mean* ± *SD*)	0.0 ± 0.0	1.6 ± 2.4	6.6 ± 6.9	0.007*	<0.001*	<0.001*
[b]Family history of stroke *n* (%)	5 (50.0)	2 (20.0)	4 (40.0)	0.510	—	—
[b]Hypertension *n* (%)	9 (90.0)	8 (80.0)	8 (80.0)	1.000	—	—
[b]Dyslipidemia *n* (%)	5 (50.0)	7 (70.0)	4 (40.0)	0.534	—	—
[b]Diabetes *n* (%)	1 (10.0)	1 (10.0)	1 (10.0)	1.000	—	—
[b]Previous stroke *n* (%)	1 (10.0)	1 (10.0)	2 (20.0)	1.000	—	—
[b]Atrial fibrillation *n* (%)	0 (00.0)	2 (20.0)	3 (30.0)	0.321	—	—
[b]Myocardial infarction *n* (%)	0 (00.0)	1 (10.0)	2 (20.0)	0.754	—	—
[b]Hypertension medication *n* (%)	9 (90.0)	8 (80.0)	7 (70.0)	0.847	—	—
[b]Diabetes medication *n* (%)	1 (10.0)	1 (10.0)	1 (10.0)	1.000	—	—
[b]Cholesterol medication *n* (%)	2 (20.0)	7 (70.0)	3 (30.0)	0.110	—	—
[b]Anticoagulant or antiplatelet *n* (%)	1 (10.0)	5 (50.0)	6 (60.0)	0.065	—	—
[b]Current smoker *n* (%)	1 (10.0)	1 (10.0)	2 (20.0)	1.000	—	—

Table 2. Clinical and demographic characteristics of subject sub-populations used for *in vitro* experiments. [a]Means compared via one-way ANOVA with subsequent planned group-wise comparisons using Bonferroni-corrected two-sample two-tailed t-test; [b]Proportions compared via 2 × 3 Fisher's exact test with subsequent planned group-wise comparisons using Bonferroni-corrected 2 × 2 Fisher's exact test; NIHSS, National Institutes of Health stroke scale; SD, standard deviation.

phytohemagglutinin-M (PHA-M) for 72 hours in the presence of pooled serum samples generated from ischemic stroke patients, neurologically asymptomatic controls, and stroke mimics (Table 2); pooled serum samples were either unmanipulated in terms of sCD163 levels or partially depleted of sCD163 using immunoprecipitation prior to treatment (Fig. 5A). Bromodexyuridine (BrdU) incorporation was monitored over the final 24 hours of stimulation and used to assess proliferation rates.

Consistent with prior reports[31], visual observations suggested decreased proliferative activity in lymphocyte cultures treated with unmanipulated ischemic stroke serum relative to those treated with unmanipulated serum from control groups, as they appeared to contain smaller and more diffuse clusters of blasting lymphocytes. However, visual indications suggested that the inhibitory effect of ischemic stroke serum was at least moderately counteracted by depletion of sCD163 (Fig. 5B). In agreement with these visual observations, we observed significantly lower levels of BrdU incorporation in lymphocytes stimulated in the presence of unmanipulated ischemic stroke serum relative to those which were stimulated in the presence of unmanipulated serum derived from control groups, an effect which was partially ablated as a result of sCD163 depletion (Fig. 5C). A second independent experiment using pooled serum samples derived from a separate subset of subjects (Supplementary Table 2) yielded similar results (Supplementary Figure 3). Taken together, these results novelly suggest that post-stroke elevations in circulating levels of sCD163 can have direct inhibitory effects on the proliferative capacity of lymphocytes.

Discussion

The primary objective of this work was to determine the role of CD163 within the context of stroke immunopathology. We hypothesized that coordinate elevations in CD163 expression and ADAM17 activity induced by stroke could drive increases in circulating levels of sCD163, which could ultimately contribute to suppression of the peripheral adaptive immune system via the known inhibitory effects of sCD163 on lymphocyte activity. Our collective findings supported this hypothesis, and suggest that sCD163 plays a novel role as a factor which synergistically links stroke-induced activation of the innate immune system and suppression of the adaptive immune system. Such a mechanism provides a unique example which suggests that the innate immune system employs protective measures aimed at mitigating the risk of post-stroke autoimmune complications driven by adaptive immune system overactivation.

Observations of elevated levels of sCD163 in the peripheral blood of ischemic stroke patients, along with the fact that these elevations were negatively associated with lymphocyte counts, provided *in vivo* associative evidence supporting our hypothesis that CD163 plays a role in modulation of the adaptive immune system following stroke. Furthermore, our *in vitro* observations suggested that this stroke-driven increase in circulating sCD163 most likely originates from activated peripheral blood monocytes, as serum from ischemic stroke patients stimulated ADAM17-dependant sCD163 production in monocyte cultures generated from the peripheral blood of healthy individuals. Our *in vitro* observations further suggested that stroke-induced elevations in circulating sCD163 have the capacity to elicit direct suppressive effects on the adaptive immune system, as depletion of sCD163 from ischemic stroke patient-derived serum was able to partially rescue its capacity to support lymphocyte proliferation. Collectively, our findings infer a mechanism in which peripherally circulating factors induced by stroke trigger ADAM17-dependant CD163 shedding by monocytes, driving an increase in sCD163 levels which act to suppress peripheral lymphocyte activity; this mechanism likely serves as a means of maintaining

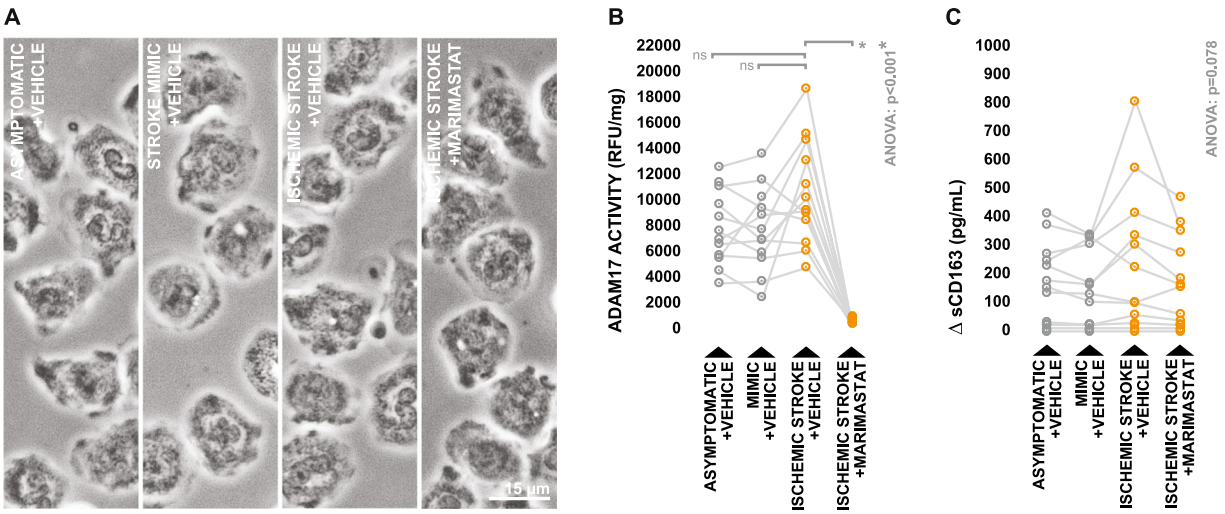

Figure 3. Effects of ischemic stroke serum on neutrophil ADAM17-dependant sCD163 production. (**A**) Morphology of healthy donor-derived neutrophils following three hours incubation with 10% serum obtained from ischemic stroke patients and control subjects, in either the presence or absence of the ADAM17 inhibitor Marimastat. (**B**) ADAM17 activity in neutrophil lysates collected following treatment. (**C**) Neutrophil-derived sCD163 levels in cell culture supernatants collected following treatment, presented as the difference in sCD163 levels observed between cell culture supernatants and serum-supplemented media incubated in the absence of cells. Means were compared via repeated measures one-way ANOVA; the Greenhouse-Geisser correction was applied to account for non-sphericity. In the case of a significant test, subsequent planned group-wise comparisons were performed using Bonferroni-corrected paired two-tailed t-test; planned comparisons are indicated by brackets.

self-tolerance as the blood brain barrier becomes disrupted and peripheral lymphoid populations become exposed to activated innate antigen presenting cells loaded with unfamiliar neural antigens (Fig. 6).

To our knowledge, our results are the first to demonstrate a direct role for the innate immune system in perpetuating stroke-induced suppression of the peripheral adaptive immune system. While our results highlighted sCD163 as a means of such cross-communication, it is likely other innate-derived factors function to mediate the adaptive immune response to stroke via similar mechanisms. This notion is accentuated by the fact that ablation of sCD163 from stroke-derived serum was not adequate to fully rescue its capacity to support lymphocyte proliferation, inferring that there are a multitude of other soluble factors present in post-stroke peripheral circulation which have similar inhibitory effects. While the origins of these factors are inevitably diverse, it is likely that some arise via a similar mechanism as sCD163, as biological mechanisms are often redundant[32]. Interesting from this regard is cluster of differentiation 14 (CD14), a membrane-bound pattern recognition receptor which is largely exclusive to the innate immune system[33,34]. Much like CD163, CD14 can be shed via a metalloproteinase-dependent mechanism to generate a soluble protein (sCD14) which has been shown to directly interact with lymphocytes and exert suppressive effects[35,36]. Preliminary results from our laboratory suggest that circulating levels of sCD14 are also elevated in response to stroke, and further exploration may reveal that sCD14 plays a similar role as sCD163 in modulation of the peripheral adaptive immune response.

While this study identified a clear role for sCD163 in stroke immunopathology in terms of its end-action, our experiments did not look to identify the soluble factors present in peripheral circulation following stroke which are responsible for triggering the shedding of CD163 from monocytes. It is plausible that this phenomenon is likely driven by a synergistic combination of stroke-induced damage associated molecules (DAMs), cytokines, and hormones, as members of the aforementioned families of factors are known to stimulate CD163 shedding. Notable from this standpoint is extracellular hemoglobin, a DAM which has been previously demonstrated as being acutely elevated in peripheral circulation following stroke as a result of intravascular and extravascular hemolysis[37]. Free hemoglobin has been characterized as a potent inducer of CD163 shedding[38], and thus, may help drive production of sCD163 in response to stroke. Along similar lines, levels of interleukin-6, cortisol, and reactive oxygen species are all known to be elevated acutely in stroke pathology[29,39,40], and all have been shown to promote sCD163 production[41,42]. Further exploration into these and other potential molecular signals which may trigger sCD163 generation within the context of stroke could not only provide a more complete picture of the mechanisms identified in this study, but a better understanding of post-stroke adaptive immune suppression as a whole, as the factors which drive post-stroke sCD163 production likely exert suppressive effects on the peripheral immune system via multiple parallel mechanisms.

While our findings are exciting, it is important to note that potentially confounding the interpretation of our results is the fact that elevations in sCD163 have been previously reported in atherosclerosis as a result of excessive intravascular macrophage activity within atherosclerotic plaques[43]. As atherosclerosis is closely linked with stroke as one of its primary pathogenic drivers[44], it leaves open the possibility that our results were atherosclerosis driven, and not by the acute event of stroke itself. However, we find this scenario unlikely, as subjects

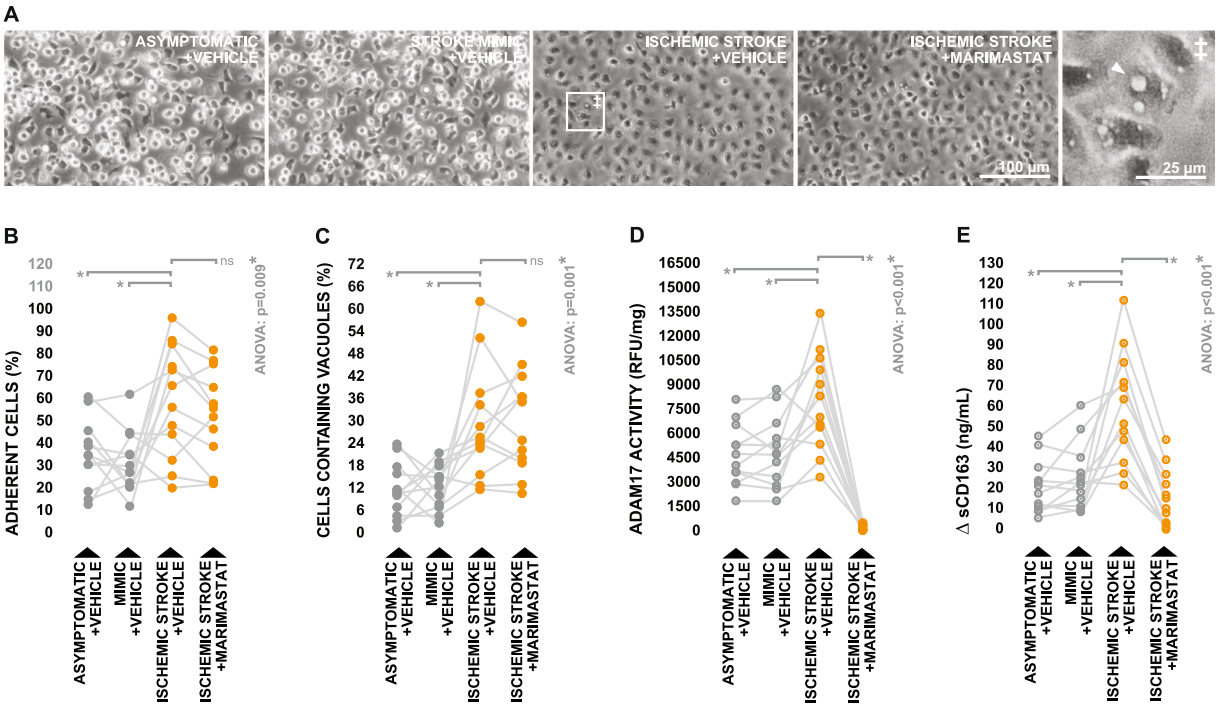

Figure 4. Effects of ischemic stroke serum on ADAM17-dependant sCD163 production by monocytes. (**A**) Morphology of healthy donor-derived monocytes following three hours incubation with 20% serum obtained from ischemic stroke patients and control subjects, in either the presence or absence of the ADAM17 inhibitor Marimastat. White arrowheads indicate cytoplasmic vacuoles. (**B–C**) Proportions of adherent monocytes and monocytes containing clearly defined vacuolar structures upon post-treatment imaging and quantification. (**D**) ADAM17 activity in monocyte lysates collected following treatment. (**E**) Monocyte-derived sCD163 levels in cell culture supernatants collected following treatment, presented as the difference in sCD163 levels observed between cell culture supernatants and serum-supplemented media incubated in the absence of cells. Means were compared via repeated measures one-way ANOVA; the Greenhouse-Geisser correction was applied to account for non-sphericity. In the case of a significant test, subsequent planned group-wise comparisons were performed using Bonferroni-corrected paired two-tailed t-test; planned comparisons are indicated by brackets.

in our control groups were relatively well matched with ischemic stroke patients in terms of the prevalence of cardiovascular disease risk factors associated with atherosclerosis. We suspect that sCD163 levels are chronically heightened with underlying cardiovascular pathology and become further elevated in response to the acute event of stroke itself. Supporting our notion that the elevations in sCD163 which we observed in ischemic stroke were a direct result of the stroke-induced neurological insult is the fact that it has recently been reported that levels of macrophage-derived sCD163 are elevated in the cerebrospinal fluid of pediatric traumatic brain injury patients[45], providing concurrent evidence that cerebral injury has the capacity to directly trigger increased sCD163 production independent of atherosclerotic pathology.

We feel it is also important to note that our exclusive use of primary human cell cultures and specimens throughout our experiments posed a unique set of challenges, and was inherently associated with experimental limitations. For example, our use of immunoprecipitation to deplete serum of CD163 in our lymphocyte proliferation experiments leaves open the possibility that the difference in proliferation rates which we observed between lymphocytes treated with CD163-depleted and CD163-normal ischemic stroke serum was driven by the removal of an off-target molecule other than CD163 via a non-specific antibody interaction. We find this scenario unlikely however, as we used a well characterized capture antibody which has been demonstrated in numerous prior investigations to have a high degree of specificity for CD163[38,46–49], and performed immunoprecipitation at low temperatures using minimal concentrations of antibody to mitigate the risk of non-specific binding events.

Another potential experimental confound lies in our use of Marimastat to inhibit ADAM17 *in vitro*; because Marimastat has activity against multiple proteases (MMP1, MMP2, MMP3, MMP7, MMP9, and MMP14 in addition to ADAM17)[50], it is possible that the ablation of stroke serum-induced monocytic sCD163 production we observed upon treatment with Marimastat was the result of the inhibition of a shedase other than ADAM17. However, we find this unlikely when considering that ADAM17 is the only known target of Marimastat which is believed to be involved in cleavage of CD163[20], and even further unlikely when considering that we observed a strong correlation between ADAM17 activity and sCD163 levels in the peripheral blood of stroke patients *in vivo*. With regards to both aforementioned cases of potential experimental confounds, it could be argued that the experimental questions at hand could have been more efficiently and definitively addressed through the genetic manipulation of CD163 and ADAM17 in a murine model of stroke; however, it is becoming increasingly evident

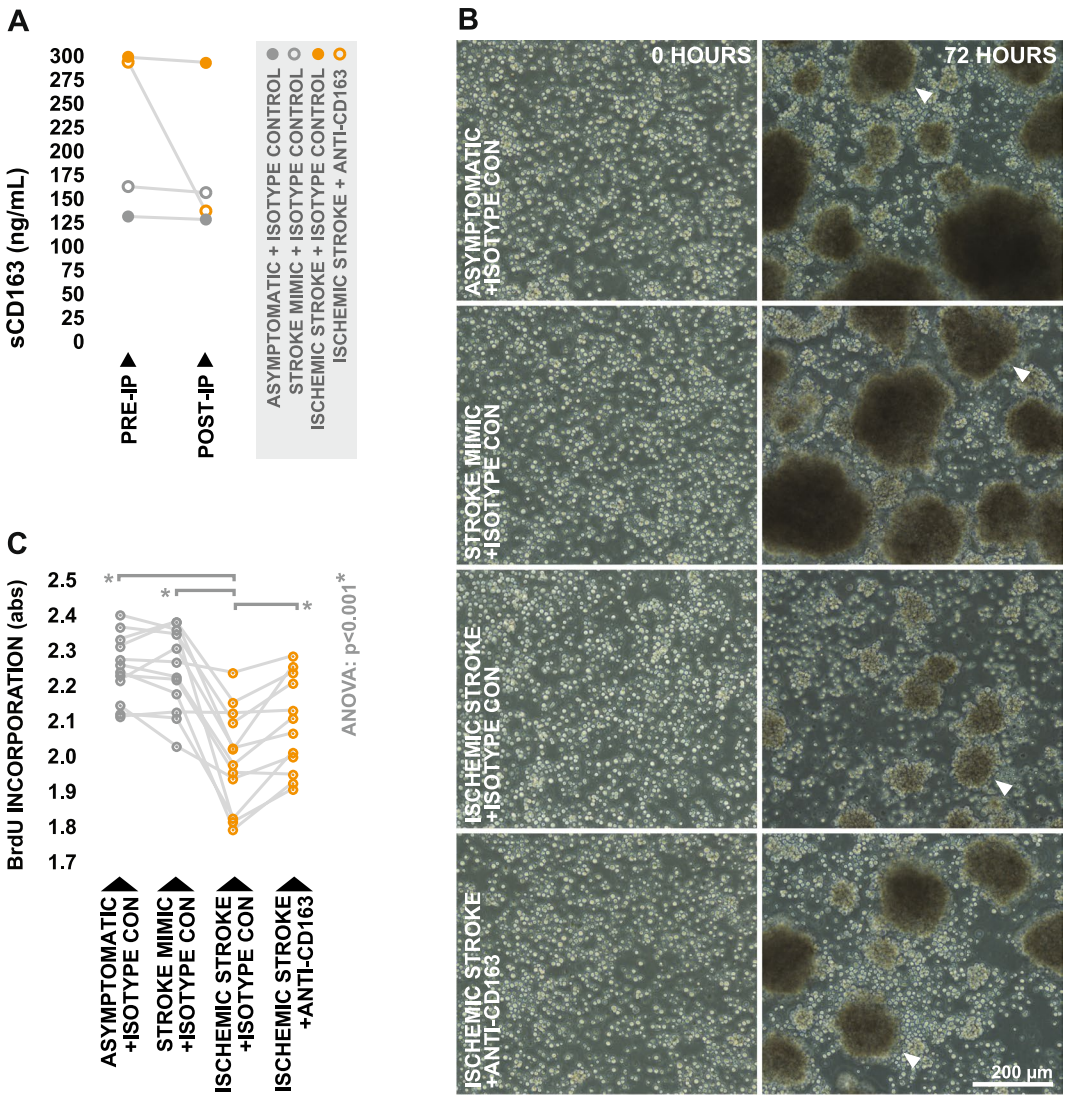

Figure 5. Influence of post-stroke peripheral blood sCD163 levels on the capacity to support lymphocyte proliferation. (**A**) Pre and post-immunoprecipitation concentrations of sCD163 in pooled serum samples obtained from ischemic stroke patients and controls, immunoprecipitated using either anti-CD163 polyclonal antibody or isotype control. (**B**) Morphology of healthy donor-derived lymphocytes following 72 hours of PHA-stimulated proliferation in the presence of 20% post-immunoprecipitation pooled serum. White arrowheads indicate clusters of blasting lymphocytes. (**C**) BrdU incorporation over the final 24 hours of treatment. Means were compared via repeated measures one-way ANOVA; the Greenhouse-Geisser correction was applied to account for non-sphericity. In the case of a significant test, subsequent planned group-wise comparisons were performed using Bonferroni-corrected paired two-tailed t-test; planned comparisons are indicated by brackets.

that experimental stroke models poorly recapitulate several aspects of pathology[51,52], and that in general, immunological responses in laboratory rodents are often poorly analogous to those in humans[53,54]. For these reasons, we feel the human-central experimental design used in this study provides tremendous translational value, in spite of the aforementioned potential limitations.

From a broader perspective, our findings are intriguing as they demonstrate a departure from the often compartmentalized view of stroke immunopathology. While there are exceptions, research regarding stroke immunopathology has long treated the adaptive and innate immune responses as independent entities, however our results and recent results of others suggest that these responses are synergistically linked via direct mechanisms. This realization is of utmost importance with regards to the current push towards the development of novel stroke therapeutics which target the peripheral immune system. Currently, experimental immune therapies are being developed which largely aim to improve stroke outcome via one of two often discrete avenues: either by inhibiting the acute innate immune response to stroke as means of limiting excessive tissue damage and mitigating the risk of negative secondary cerebrovascular events such as edema and hemorrhagic transformation[55–57], or by post-acutely stimulating the peripheral adaptive immune system as a means of limiting the risk of complications induced by post-stroke infection[58–61]. However, immunotherapeutics proposed along this line of thinking often

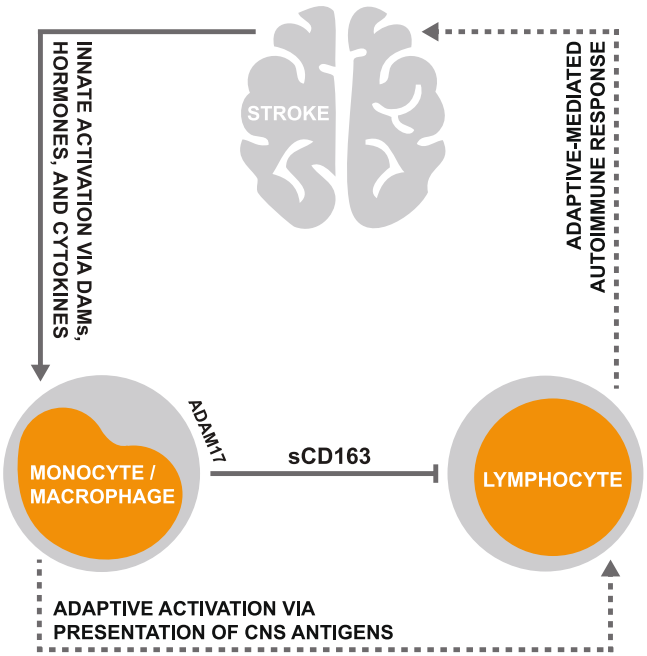

Figure 6. Proposed role for CD163 in modulation of the stroke-induced peripheral immune response. Stroke-driven elevations in circulating levels of damage associated molecules (DAMs), proinflammatory cytokines, and hormones coordinately trigger innate immune system activation and ADAM17-dependant CD163 shedding by monocytes, resulting in increased generation of sCD163. Heightened circulating sCD163 levels subsequently act to suppress lymphocyte activity, likely as a means of limiting the risk of a CNS-directed autoimmune response resulting from adaptive immune system activation.

fail to account the possible interplay between the adaptive and innate immune systems, and the potential repercussions that could stem from modulating one response without consideration for the other.

A perfect example in this regard is the fact that ADAM17 inhibitors are often cited as a potential stroke therapeutic under the premise that they could ultimately limit excessive innate-driven inflammation and its associated complications via a reduction in TNFα production[62–65]. However, our results clearly demonstrate that inhibition of ADAM17 within the innate immune system could directly interfere with mechanisms which act to suppress the adaptive immune system, an unintended effect which could put patients at elevated risk for the development of long-term autoimmune complications associated with loss of CNS self-tolerance. Such an example highlights the necessity for a global view regarding the peripheral immune system in terms of the development of novel stroke immunotherapeutics. Unfortunately, therapeutic design from such a perspective is currently unrealistic, as the mechanisms which drive the stroke-induced peripheral immune response, particularly that of the adaptive immune system, are still largely unknown. This current gap in knowledge may underlie the reality that stroke immunotherapeutics have thus-far been largely unsuccessful[66]. Further future work which aims to characterize the peripheral immune response to stroke and its underlying mechanisms from a panoptic systems biology approach, preferably within human-centric models, would likely generate the foundational basis for the development of stroke immunotherapeutics with higher chances for clinical success.

Collectively, our results demonstrate a novel role for CD163 as factor which mechanistically couples stroke induced-activation of the peripheral innate immune system and suppression of the peripheral adaptive immune system. Our results provide a unique example which suggests that the innate immune system employs protective mechanisms aimed at mitigating the risk of post-stroke autoimmune complications driven by adaptive immune system overactivation. Further work which looks to characterize similar pathways of cross-communication between the innate and adaptive immune systems within the context of stroke would likely provide a better understanding of stroke pathology as a whole, and allow for more informed development of stroke-targeted immunotherapeutics.

Methods

Patients. Acute ischemic stroke patients, acute stroke mimics, and neurologically asymptomatic controls were recruited at Ruby Memorial Hospital, Morgantown, WV. Ischemic stroke patients displayed definitive radiographic evidence of vascular ischemic pathology on magnetic resonance imaging (MRI) or computed tomography (CT) according to the established criteria for diagnosis of acute ischemic cerebrovascular syndrome (AICS)[67], and diagnoses were confirmed by an experienced neurologist. Patients admitted to the emergency department as suspected strokes based on the overt presentation of stroke-like symptoms, but receiving a definitive negative diagnosis for stroke upon neuroradiological imaging and clinical evaluation were identified as acute stroke mimics[67]. Discharge diagnoses of stroke mimics included cases of seizures, complex migraines, hypertensive encephalopathy, and other non-stroke conditions which induce neurological symptoms. Prospective subjects

were excluded if they received a non-definitive diagnosis, displayed evidence of hemorrhagic pathology, presented with cancer as a co-pathology, reported a prior hospitalization within 90 days, or were under 18 years of age. Blood was sampled within 24 hours of onset, as determined by the time the patient was last known to be free of stroke-like symptoms. In the case of patients who received thrombolytic therapy, blood samples were collected prior to the administration of recombinant tissue plasminogen activator (rtPA). Injury severity was determined according to the NIHSS at the time of blood draw. Control subjects were deemed neurologically normal by a trained neurologist at the time of enrolment. Demographic information was collected from either the subject or significant other by a trained clinician. Procedures were approved by the institutional review boards of West Virginia University and Ruby Memorial Hospital (IRB protocol 1410450461R001), and all experiments were performed in accordance with relevant guidelines and regulations. Written informed consent was obtained from all subjects or their authorized representatives prior to study procedures.

Neuroradiological imaging. Neuroradiological imaging was performed using either MRI or CT within 24 hours of symptom onset. CT imaging was performed on either a Toshiba Aquilion 64 or Toshiba Aquilion 320 scanner (5 mm slices acquired at 120 KVp, 250 mA). MRI imaging was performed using either a Siemens Aera or Siemens Verio scanner (5 mm slices, 5 mm inter-slice gap, acquired via diffusion-weighted echoplanar imaging with a B-factor of 1000 s/mm^2). The BrainLAB iPlan Neuroradiology software package (BrainLAB, Westchester, Ill) was used to calculate infarct volume via manual tracing, and all infarct volume calculations were verified by an experienced neurologist.

Blood collection. Parallel peripheral venous whole blood samples were collected from subjects via PAXgene RNA tubes (Qiagen, Valencia, CA), K_2 EDTA Vacutainers (Becton Dickenson, Franklin Lakes, NJ), and serum separator tubes (Becton Dickenson). PAXgene RNA tubes were frozen immediately and stored at −80 °C until RNA extraction. K_2 EDTA tubes were stored at room temperature until white blood cell differential (less than 30 minutes), plasma isolation (less than 30 minutes), or leukocyte isolation (performed immediately). Serum separator tubes were stored at room temperature until serum isolation (less than 30 minutes).

Isolation of serum and plasma. For plasma isolation, EDTA-treated blood was spun at 2,000 * g for 10 minutes to sediment hemocytes. Plasma was collected for ELISA, and the total hemocyte fraction was retained for subsequent protein extraction and ADAM17 activity assay. Plasma was additionally spun at 10,000 * g for 10 minutes to remove any residual blood cells or debris. For serum isolation, serum separator tubes were incubated at room temperature for a minimum of 15 minutes to allow for coagulation, and subsequently spun at 2,000 * g for 10 minutes to sediment the resulting thrombus. Resultant samples were stored at −80 °C until analysis.

RNA extraction and quantitative reverse transcription PCR. Whole blood RNA was extracted from PAXgene tubes via the PreAnalytiX PAXgene blood RNA kit (Qiagen) and automated using the QIAcube system (Qiagen). Quantity and purity of isolated RNA was determined via spectrophotometry (NanoDrop, Thermo Scientific, Waltham, MA). cDNA was generated from purified RNA using the Applied Biosystems high capacity reverse transcription kit. For qPCR, target sequences were amplified from 10 ng of cDNA input using sequence specific primers (Supplementary Table 3) and detected via SYBR green (PowerSYBR, Thermo-Fisher) on the RotorGeneQ thermocycling system (Qiagen). All reactions were performed in triplicate. Raw amplification plots were background corrected and CT values were generated via the RotorGeneQ software package. Transcripts of *B2M*, *PPIB*, and *ACTB* were amplified as references and normalization was performed using the NORMA-Gene data-driven normalization algorithm as described previously[68,69]. Statistical testing was performed using normalized CT values, and data were linearly transformed and scaled relative to the mean of the control group for visual representation per the methodology described by Schittgen and Livak[70].

White blood cell differential. Complete blood count was obtained from EDTA-treated blood via combined optical flow cytometry and cellular impedance using an automated clinical hematology analyzer (Cell-Dyn, Abbott Diagnostics, Santa Clara, CA).

Isolation of primary leukocytes for cell culture. Starting with 30 mLs of healthy donor-derived EDTA-treated blood, peripheral blood mononuclear cells (PBMCs) were separated from polymorphonuclear cells (PMNs) and red blood cells (RBCs) via centrifugation over a polysaccharide-sodium diatrizoate density gradient (Lymphoprep, 1.077 g/mL, StemCell Technologies) for 30 minutes at 400 * g. Resultant interphase PBMC fractions were collected, resuspended in RPMI 1640 (Life Technologies, Grand Island, NY) containing 10% autologous serum, separated into two aliquots, and set aside at room temperature. Pelleted PMN/RBCs were immediately placed on ice for PMN enrichment via RBC lysis induced by two 5 minute incubations with a 1:10 volume of ice cold ammonium chloride (ACK) buffer. The resultant PMNs were rinsed in ice cold phosphate buffered saline (PBS), counted via automated cytometer (Cellmeter × 1, Nexcelom Bioscience, Lawrence, MA), and immediately plated for experiments.

Following PNM isolation, monocytes were further enriched from one aliquot of PBMCs via a second round of density gradient centrifugation as described by Menck *et al.*[71]. Briefly, PBMC suspensions were layered over an iso-osmotic 46% Percoll (1.131 g/mL, Sigma Aldrich) solution prepared in RPMI 1640 containing 10% autologous serum and centrifuged at 500 * g for 30 minutes. Monocytes were collected from the resultant interphase, rinsed in PBS, counted, and immediately plated for experiments.

Following PMN and monocyte isolation, the remaining aliquot of PBMCs was rinsed in PBS and seeded in T75 flasks for lymphocyte expansion. Lymphocytes were expanded for 72 hours under standard mammalian cell

culture conditions in a growth media comprised of RPMI 1640 containing 2% PHA-M (Gibco, Grand Island, NY), 2 mM L-Alanyl-Glutamine (GlutaMAX, Gibco), 25 mM HEPES (Gibco), 50 uM BME (Gibco), and 1% antibiotic-antimycotic (Gibco), supplemented with 10% autologous serum. Following expansion, actively proliferating lymphocytes were rinsed in PBS, counted, and plated for experiments.

Neutrophil culture. Neutrophils from healthy donors were seeded in 12-well plates at a density of $7.5 * 10^5$ cells per well in 250 uL of GlutaMax-supplemented RPMI 1640 containing 10% patient serum along with either Marimastat (10 uM, Sigma Aldrich, St-Louis, MO) or vehicle (DMSO, Fisher Scientific). Following three hours of incubation under standard mammalian culture conditions, cells were lysed in NP40 lysis buffer (Life Technologies) and cellular ADAM17 activity was assessed via enzyme activity assay. Cell culture supernatants were collected and concentrations of sCD163 were quantified via ELISA; levels of neutrophil-derived sCD163 were determined by subtracting the concentration of sCD163 in media incubated without cells from the concentrations of sCD163 observed in cell culture supernatants.

Monocyte culture. Monocytes from healthy donors were seeded in 12-well plates at a density of $1 * 10^6$ cells per well in 250 uL of GlutaMax-supplemented RPMI 1640 containing 20% patient serum along with either Marimastat (10 uM) or vehicle (DMSO). Following three hours of incubation under standard mammalian culture conditions, cells were lysed in NP40 lysis buffer and cellular ADAM17 activity was assessed via enzyme activity assay. Cell culture supernatants were collected and concentrations of sCD163 were quantified via ELISA; levels of monocytes-derived sCD163 were determined by subtracting the concentration of sCD163 in media incubated without cells from the concentrations of sCD163 observed in cell culture supernatants.

sCD163 depletion from human serum. sCD163 was depleted from pooled serum samples via immunoprecipitation using biotinylated goat polyclonal antibody raised against the extracellular region of CD163 (AF1607, R&D Systems, Minneapolis, MN). Biotinylated normal goat IgG (AF108, R&D Systems) was used as an isotype immunoprecipitation control. Immunoglobulins were conjugated to polymer-coated superparamagnetic beads (Dynabeads Streptavidin T1, Thermo Fisher, Waltham MA) at a ratio of 10 ug of immunoglobulins per 1 mg of beads. For immunoprecipitation, 5 mL of pooled serum was precleared with normal IgG conjugated beads, and then incubated with 0.5 mg of either normal IgG conjugated beads or anti-CD163 conjugated beads for 30 minutes at 4 °C. Beads were subsequently separated from serum samples via multiple rounds of magnetic separation. Immunoprecipitation was performed under aseptic conditions and serum was filtered at 14 microns following immunoprecipitation to remove potential microbial contaminants prior to cell culture. Depletion of sCD163 was subsequently confirmed via ELISA.

Lymphocyte proliferation assay. Expanded lymphocytes from healthy donors were seeded in 48 well plates at $5*10^4$ cell per well in 200 uL growth media supplemented 20% pooled patient serum. Following 48 hours of culture, BrdU (Roche Life Sciences, Indianapolis, IN) was added to cultures at a final concentration of 20 uM. After allowing for 24 hours for BrdU incorporation, lymphocytes were adhered via centrifugation and fixed for BrdU quantification. Incorporated BrdU was quantified via colorimetric ELISA (Roche Life Sciences) per manufacture instructions.

sCD163 ELISA. sCD163 was measured in plasma samples and cell culture supernatants using a commercially available colorimetric ELISA assay (RAB0082, Sigma-Aldrich). Plasma samples were diluted 1:50, neutrophil cell culture supernatants were diluted 1:5, and monocyte cell culture supernatants were diluted 1:10 prior to analysis. Absorbance readings were obtained using the Synergy HT multi-mode microplate reader (BioTek, Winooski VT). Due to the potential confound of hemolysis on concentrations of leukocyte derived analytes, plasma samples were screened for hemolysis prior to ELISA. Plasma absorbance was measured at 385 and 414 nm via spectrophotometry (NanoDrop, Thermo Scientific, Waltham, MA) and used to calculate a hemolysis score as described by Appierto *et al.*[72]. Plasma samples with detectable hemolysis were excluded from analysis.

ADAM17 activity assay. Total hemocyte fractions were thawed, mixed with NP-40 lysis buffer (Thermo Fisher) at a 1 to 1 ratio, and depleted of hemoglobin via the HemogloBind hemoglobin removal kit (Biotech Support Group, Monmouth Junction, NJ) as described by Park *et al.*[73]. Protein concentrations of hemoglobin-depleted total hemocyte lysates and cell culture lysates were determined via DC-protein assay (Bio-Rad, Hercules, CA). ADAM17 activity was measured in 200 ug of total hemocyte lysate, or 10 ug of cell culture lysate, via the InnoZyme fluorometric TACE activity kit (EMD Millipore, Temecula, CA) per manufacture instructions. Fluorometric readings were obtained using the Synergy HT multi-mode microplate reader (BioTek). Due to the reversible nature of ADAM17 inhibition by Marimastat, experimental concentrations of drug were maintained in assay buffers when testing samples from inhibitor-treated conditions.

Phase contrast microscopy and image-based morphological quantification. Phase contrast images of primary leukocyte cultures were obtained from an AxioObserver inverted microscope (Ziess, Thornwood, NY) equipped with a AxioCam mR5 digital camera (Ziess) using the AxioVision imaging software suite (Ziess). Scale bars were generated via imaging of a 0.07–1.50 mm scale calibration slide (Motic, Richmond, BC, CA).

A basic point-counting system was used for image-based morphological quantification of monocyte cultures. Three randomly selected images from each culture were overlaid with a 9×12 grid. Each intersecting point of the grid (108 points per image) was assessed for the presence of a cell; if a cell was present, it was determined whether it was adherent, as well as whether it contained clearly defined internal vacuolar structures. The percentage of

adherent cells, as well as the percentage of cells containing vacuoles, was than calculated, both relative to the total number of cells analyzed. Images were analyzed in random order and counters were blinded to experimental information.

Statistical analysis and data availability. Statistics were performed using SPSS (IBM, Chicago, Ill) in combination with R 2.14 (R project for statistical computing)[74] via the SPSS R integration plug-in. Fisher's exact test was used for comparison of dichotomous variables. Student t-test, one-way ANOVA, one-way ANCOVA, or repeated measures one-way ANOVA was used for comparison of continuous variables where appropriate. In some instances of ANCOVA and one-way ANOVA, data were log-transformed prior to analysis in order to meet normality and homogeneity of variance assumptions, which were evaluated via the Shapiro-Wilk test and Levene's test. In some instances of repeated measures one-way ANOVA, values were adjusted via the Greenhouse-Geisser correction to account for non-sphericity, which was assessed using Mauchly's test. Either Spearman's rho or Pearson's r was used to assess the strength of correlational relationships where appropriate based on level of homoscedasticity. Principle components analysis was used for dimensionality reduction; prior to analysis, data were tested for sphericity and sampling adequacy via Bartlett's test and the Kaiser-Mayer-Olkin index. The level of significance was established at 0.05 for all statistical testing. In the cases of multiple comparisons, p-values were adjusted using Bonferroni correction. Parameters of all statistical tests performed are outlined in detail within the figure legends. The datasets generated and analyzed during this study are available from the corresponding author upon reasonable request.

References

1. Urra, X. *et al*. Monocytes are major players in the prognosis and risk of infection after acute stroke. *Stroke* **40**, 1262–1268 (2009).
2. Vogelgesang, A. *et al*. Analysis of lymphocyte subsets in patients with stroke and their influence on infection after stroke. *Stroke* **39**, 237–241 (2008).
3. Urra, X., Cervera, Á. & Villamor, N. Planas, a. M. & Chamorro, Á. Harms and benefits of lymphocyte subpopulations in patients with acute stroke. *Neuroscience* **158**, 1174–1183 (2009).
4. Harms, H. *et al*. Preventive antibacterial therapy in acute ischemic stroke: A randomized controlled trial. *PLoS One* **3** (2008).
5. Planas, A. M. *et al*. Brain-Derived Antigens in Lymphoid Tissue of Patients with Acute Stroke. *J. Immunol.* **188**, 2156–2163 (2012).
6. Becker, K. Autoimmune Responses to Brain FollowingStroke. *Transl. Stroke Res.* **3**, 310–317 (2012).
7. Becker, K. J. *et al*. Autoimmune responses to the brain after stroke are associated with worse outcome. *Stroke* **42**, 2763–2769 (2011).
8. Koennecke, H.-C. *et al*. Factors influencing in-hospital mortality and morbidity in patients treated on a stroke unit. *Neurology* **77**, 965–972 (2011).
9. Vernino, S. *et al*. Cause-specific mortality after first cerebral infarction: A population-based study. *Stroke* **34**, 1828–1832 (2003).
10. Kimura, K., Minematsu, K., Kazui, S. & Yamaguchi, T. Mortality and Cause of Death after Hospital Discharge in 10,981 Patients with Ischemic Stroke and Transient Ischemic Attack. *Cerebrovasc. Dis.* **19**, 171 (2005).
11. Katzan, I. L., Cebul, R. D., Husak, S. H., Dawson, N. V. & Baker, D. W. The effect of pneumonia on mortality among patients hospitalized for acute stroke. *Neurology* **60**, 620–625 (2003).
12. Brooks, S. D. *et al*. Admission neutrophil-lymphocyte ratio predicts 90 day outcome after endovascular stroke therapy. *J. Neurointerv. Surg*. 1–6, https://doi.org/10.1136/neurintsurg-2013-010780 (2013).
13. Prass, K. *et al*. Stroke-induced immunodeficiency promotes spontaneous bacterial infections and is mediated by sympathetic activation reversal by poststroke T helper cell type 1-like immunostimulation. *J. Exp. Med.* **198**, 725–736 (2003).
14. Hilker, R. *et al*. Nosocomial pneumonia after acute stroke: Implications for neurological intensive care medicine. *Stroke* **34**, 975–981 (2003).
15. Davenport, R. J., Dennis, M. S., Wellwood, I. & Warlow, C. P. Complications After Acute Stroke. *Stroke* **27**, 415–420 (1996).
16. Johnston, K. C. *et al*. Medical and neurological complications of ischemic stroke: experience from the RANTTAS trial. RANTTAS Investigators. *Stroke* **29**, 447–453 (1998).
17. Schaer, D. J. *et al*. CD163 is the macrophage scavenger receptor for native and chemically modified hemoglobins in the absence of haptoglobin. *Blood* **107**, 373–80 (2006).
18. Lau, S. K., Chu, P. G. & Weiss, L. M. CD163: A Specific Marker of Macrophages in Paraffin-Embedded Tissue Samples. *Am. J. Clin. Pathol.* **122**, 794–801 (2004).
19. Cunnington, A. J. *et al*. Prolonged neutrophil dysfunction after Plasmodium falciparum malaria is related to hemolysis and heme oxygenase-1 induction. *J. Immunol.* **189**, 5336–46 (2012).
20. Etzerodt, A., Maniecki, M. B., Møller, K., Møller, H. J. & Moestrup, S. K. Tumor necrosis factor α-converting enzyme (TACE/ADAM17) mediates ectodomain shedding of the scavenger receptor CD163. *J. Leukoc. Biol.* **88**, 1201–1205 (2010).
21. Etzerodt, A. *et al*. Structural basis for inflammation-driven shedding of CD163 ectodomain and tumor necrosis factor-?? in macrophages. *J. Biol. Chem.* **289**, 778–788 (2014).
22. Frings, W., Dreier, J. & Sorg, C. Only the soluble form of the scavenger receptor CD163 acts inhibitory on phorbol ester-activated T-lymphocytes, whereas membrane-bound protein has no effect. *FEBS Lett.* **526**, 93–6 (2002).
23. Högger, P. & Sorg, C. Soluble CD163 inhibits phorbol ester-induced lymphocyte proliferation. *Biochem. Biophys. Res. Commun.* **288**, 841–3 (2001).
24. Timmermann, M., Buck, F., Sorg, C. & Högger, P. Interaction of soluble CD163 with activated T lymphocytes involves its association with non-muscle myosin heavy chain type A. *Immunol. Cell Biol.* **82**, 479–487 (2004).
25. O'Connell, G. C. *et al*. Machine-learning approach identifies a pattern of gene expression in peripheral blood that can accurately detect ischaemic stroke. *npj Genomic Med.* **1**, 16038 (2016).
26. Cardenas, A. *et al*. Upregulation of TACE/ADAM17 after ischemic preconditioning is involved in brain tolerance. *J Cereb Blood Flow Metab* **22**, 1297–1302 (2002).
27. Katakowski, M. *et al*. Stroke-induced subventricular zone proliferation is promoted by tumor necrosis factor-alpha-converting enzyme protease activity. *J. Cereb. Blood Flow Metab.* **27**, 669–78 (2007).
28. Romera, C. *In Vitro* Ischemic Tolerance Involves Upregulation of Glutamate Transport Partly Mediated by the TACE/ADAM17-Tumor Necrosis Factor- Pathway. *J. Neurosci.* **24**, 1350–1357 (2004).
29. Castellanos, M. *et al*. Inflammation-Mediated Damage in Progressing Lacunar Infarctions. *Stroke* **33**, 982–987 (2002).
30. Sotgiu, S. *et al*. Inflammatory biomarkers in blood of patients with acute brain ischemia. *Eur. J. Neurol.* **13**, 505–513 (2006).
31. Kostić, V., Mostarica-Stojković, M., Ramić, Z., Kovàcević, M. & Lukić, M. Serum immunoinhibitory factors in stroke patients. *Eur. Neurol.* **28**, 331–4 (1988).
32. Tononi, G., Sporns, O. & Edelman, G. M. Measures of degeneracy and redundancy in biological networks. *Proc.Natl.Acad.Sci.,USA* **96**, 3257–3262 (1999).

33. Maliszewski, C. R. *et al*. Isolation and characterization of My23, a myeloid cell-derived antigen reactive with the monoclonal antibody {AML-2-23}. *J. Immunol. {(Baltimore,} Md. 1950)* **135**, 1929–1936 (1985).
34. Pugin, J. *et al*. CD14 is a pattern recognition receptor. *Immunity* **1**, 509–516 (1994).
35. Rey Nores, J. E. *et al*. Soluble CD14 acts as a negative regulator of human T cell activation and function. *Eur. J. Immunol.* **29**, 265–276 (1999).
36. Bazil, V. *et al*. Biochemical characterization of a soluble form of the 53-kDa monocyte surface antigen. *Eur. J. Immunol.* **16**, 1583–9 (1986).
37. Huang, P. *et al*. Serum free hemoglobin as a novel potential biomarker for acute ischemic stroke. *J. Neurol.* **256**, 625–31 (2009).
38. Subramanian, K., Du, R., Tan, N. S., Ho, B. & Ding, J. L. CD163 and IgG codefend against cytotoxic hemoglobin via autocrine and paracrine mechanisms. *J. Immunol.* **190**, 5267–78 (2013).
39. Olsson, T., Astrom, M., Eriksson, S. & Forssell, A. Hypercortisolism revealed by the dexamethasone suppression test in patients [corrected] with acute ischemic stroke. *Stroke* **20**, 1685–1690 (1989).
40. Nanetti, L. *et al*. Reactive oxygen species plasmatic levels in ischemic stroke. *Mol. Cell. Biochem.* **303**, 19–25 (2007).
41. Timmermann, M. & Högger, P. Oxidative stress and 8-iso-prostaglandin F(2alpha) induce ectodomain shedding of CD163 and release of tumor necrosis factor-alpha from human monocytes. *Free Radic. Biol. Med.* **39**, 98–107 (2005).
42. Buechler, C. *et al*. Regulation of scavenger receptor CD163 expression in human monocytes and macrophages by pro- and antiinflammatory stimuli. *J. Leukoc. Biol.* **67**, 97–103 (2000).
43. Aristoteli, L. P., Møller, H. J., Bailey, B., Moestrup, S. K. & Kritharides, L. The monocytic lineage specific soluble CD163 is a plasma marker of coronary atherosclerosis. *Atherosclerosis* **184**, 342–347 (2006).
44. Arenillas, J. F. Intracranial atherosclerosis: Current concepts. *Stroke* **42** (2011).
45. Newell, E. *et al*. Cerebrospinal Fluid Markers of Macrophage and Lymphocyte Activation After Traumatic Brain Injury in Children. *Pediatr. Crit. care Med.* **16**, 549–57 (2015).
46. Van Gorp, H., Van Breedam, W., Van Doorsselaere, J., Delputte, P. L. & Nauwynck, H. J. Identification of the CD163 protein domains involved in infection of the porcine reproductive and respiratory syndrome virus. *J. Virol.* **84**, 3101–5 (2010).
47. Caì, Y. *et al*. Simian hemorrhagic fever virus cell entry is dependent on CD163 and uses a clathrin-mediated endocytosis-like pathway. *J. Virol.* **89**, 844–56 (2015).
48. Zizzo, G., Hilliard, B. A., Monestier, M. & Cohen, P. L. Efficient clearance of early apoptotic cells by human macrophages requires M2c polarization and MerTK induction. *J. Immunol.* **189**, 3508–20 (2012).
49. Klatt, N. R. *et al*. Availability of activated CD4+ T cells dictates the level of viremia in naturally SIV-infected sooty mangabeys. *J. Clin. Invest.* **118**, 2039–49 (2008).
50. Rasmussen, H. S. & McCann, P. P. Matrix metalloproteinase inhibition as a novel anticancer strategy: a review with special focus on batimastat and marimastat. *Pharmacol. Ther.* **75**, 69–75 (1997).
51. Mergenthaler, P. & Meisel, A. Do stroke models model stroke? *Dis. Model. Mech.* **5**, 718–25 (2012).
52. Sharp, F. R. & Jickling, G. C. Modeling immunity and inflammation in stroke: differences between rodents and humans? *Stroke* **45**, e179–e180 (2014).
53. Mestas, J. & Hughes, C. C. W. Of mice and not men: differences between mouse and human immunology. *J. Immunol.* **172**, 2731–8 (2004).
54. Seok, J. *et al*. Genomic responses in mouse models poorly mimic human inflammatory diseases. *Proc. Natl. Acad. Sci. USA* **110**, 3507–3512 (2013).
55. Krams, M. *et al*. Acute Stroke Therapy by Inhibition of Neutrophils (ASTIN): An Adaptive Dose-Response Study of UK-279,276 in Acute Ischemic Stroke. *Stroke* **34**, 2543–2548 (2003).
56. Investigators Enlimomab Acute Stroke Trial. Use of anti-ICAM-1 therapy in ischemic stroke: results of the Enlimomab Acute Stroke Trial. *Neurology* **57**, 1428–34 (2001).
57. del Zoppo, G. J. Acute anti-inflammatory approaches to ischemic stroke. *Ann. N. Y. Acad. Sci.* **1207**, 143–148 (2010).
58. Meisel, C. & Meisel, A. Suppressing immunosuppression after stroke. *N. Engl. J. Med.* **365**, 2134–6 (2011).
59. Zhang, B. *et al*. Estradiol and G1 reduce infarct size and improve immunosuppression after experimental stroke. *J. Immunol.* **184**, 4087–4094 (2010).
60. Maier, I. L., Karch, A., Mikolajczyk, R., Bähr, M. & Liman, J. Effect of beta-blocker therapy on the risk of infections and death after acute stroke - A historical cohort study. *PLoS One* **10**, 1–10 (2015).
61. Smith, C. J. *et al*. Interleukin-1 receptor antagonist reverses stroke-associated peripheral immune suppression. *Cytokine* **58**, 384–389 (2012).
62. Green, A. R. & Shuaib, A. Therapeutic strategies for the treatment of stroke. *Drug Discov. Today* **11**, 681–693 (2006).
63. Tuttolomondo, A., Pecoraro, R. & Pinto, A. Studies of selective TNF inhibitors in the treatment of brain injury from stroke and trauma: a review of the evidence to date. *Drug Des Devel Ther* **8**, 2221–2238 (2014).
64. Green, A. R. Pharmacological approaches to acute ischaemic stroke: reperfusion certainly, neuroprotection possibly. *Br. J. Pharmacol.* **153**(Suppl), S325–38 (2008).
65. Arribas, J. & Esselens, C. ADAM17 as a therapeutic target in multiple diseases. *Curr. Pharm. Des.* **15**, 2319–35 (2009).
66. Amantea, D. *et al*. Rational modulation of the innate immune system for neuroprotection in ischemic stroke. *Front. Neurosci.* **9**, 1–20 (2015).
67. Kidwell, C. S. & Warach, S. Acute Ischemic Cerebrovascular Syndrome: Diagnostic Criteria. *Stroke* **34**, 2995–2998 (2003).
68. Heckmann, L.-H., Sørensen, P. B., Krogh, P. H. & Sørensen, J. G. NORMA-Gene: a simple and robust method for qPCR normalization based on target gene data. *BMC Bioinformatics* **12**, 250 (2011).
69. O'Connell, G. C. *et al*. Leukocyte Dynamics Influence Reference Gene Stability in Whole Blood: Data-Driven qRT-PCR Normalization Is a Robust Alternative for Measurement of Transcriptional Biomarkers. *Lab. Med.* **48**, https://doi.org/10.1093/labmed/lmx035 *in press* (2017).
70. Schmittgen, T. D. & Livak, K. J. Analyzing real-time PCR data by the comparative C T method. *Nat. Protoc.* **3**, 1101–1108 (2008).
71. Menck, K. *et al*. Isolation of human monocytes by double gradient centrifugation and their differentiation to macrophages in teflon-coated cell culture bags. *J. Vis. Exp.* e51554 (2014).
72. Appierto, V. *et al*. A lipemia-independent NanoDrop(®)-based score to identify hemolysis in plasma and serum samples. *Bioanalysis* **6**, 1215–26 (2014).
73. Park, K., Saudek, C. D. & Hart, G. W. Increased expression of beta-N-acetylglucosaminidase in erythrocytes from individuals with pre-diabetes and diabetes. *Diabetes* **59**, 1845–50 (2010).
74. Ross, I., Robert, G., Ihaka, R. & Gentleman, R. R: A Language for Data Analysis and Graphics. *Journal of computational and graphical statistics* **5**, 299–314 (1996).

Acknowledgements

The authors would foremost like to thank the subjects and their families, as this work was truly made possible by their selfless contribution. We would further like to thank the stroke team at Ruby Memorial Hospital for their support. In addition, we would like to thank Dr. Daniel Laskowitz (Duke University), Dr. Jason Huber (West Virginia University), Dr. Lori Hazlehurst (West Virginia University), and Dr. Gordon Meares (West Virginia

University) for critical review of the manuscript. Finally, we would like to thank Dr. Ashley Petrone (West Virginia University) and Dr. Asano Shinichi (West Virginia University) for general laboratory assistance. Work was funded via a Robert Wood Johnson Foundation Nurse Faculty Scholar award to TLB (70319) and a National Institutes of Health CoBRE sub-award to TLB (P20 GM109098).

Author Contributions

Work was conceptualized by G.C.O. Clinical sample collection and recruitment of human subjects was performed by N.L.-W. and C.S.T., and overseen by P.D.C. and T.L.B. Analysis of neuroradiological imaging was performed by Y.K. and A.R.T. Molecular experiments were designed and performed by G.C.O. Data were analyzed by G.C.O. Manuscript was written by G.C.O. with contributions from N.L.-W., C.S.T., Y.K., A.R.T., P.D.C. and T.L.B.

Additional Information

Supplementary information accompanies this paper at https://doi.org/10.1038/s41598-017-13291-6.

Competing Interests: G.C.O. and T.L.B. have a patent pending re: genomic patterns of expression for stroke diagnosis. T.L.B. serves as chief scientific officer for Valtari Bio Incorporated. Work by G.C.O. is part of a pending licensing agreement with Valtari Bio Incorporated. The remaining authors report no potential conflicts of interest.

Publisher's note: Springer Nature remains neutral with regard to jurisdictional claims in published maps and institutional affiliations.